the plant journal

SEB SOCIETY FOR EXPERIMENTAL BIOLOGY

The Plant Journal (2009) **59**, 123–135 doi: 10.1111/j.1365-313X.2009.03860.x

AtMBD9 modulates Arabidopsis development through the dual epigenetic pathways of DNA methylation and histone acetylation

Mahmoud W. F. Yaish, Mingsheng Peng[†] and Steven J. Rothstein[*]

Department of Molecular and Cellular Biology, University of Guelph, Guelph, ON, N1G 2W1, Canada

Received 21 October 2008; revised 17 February 2009; accepted 24 February 2009; published online 27 March 2009.
[*]For correspondence (fax 1 519 837 1802; e-mail rothstei@uoguelph.ca).
[†]Present address: Monsanto Company, 700 Chesterfield Parkway West, Chesterfield, MO 63017, USA.

SUMMARY

Mutations within the Arabidopsis *METHYL-CpG BINDING DOMAIN 9* gene (*AtMBD9*) cause pleotropic phenotypes including early flowering and multiple lateral branches. Early flowering was previously attributed to the repression of flowering locus C (*FLC*) due to a reduction in histone acetylation. However, the reasons for other phenotypic variations remained obscure. Recent studies suggest an important functional correlation between DNA methylation and histone modifications. By investigating this relationship, we found that the global genomic DNA of *atmbd9* was over-methylated, including the *FLC* gene region. Recombinant AtMBD9 does not have detectable DNA demethylation activity *in vitro*, but instead has histone acetylation activity. Ectopic over-expression of *AtMBD9* and transient DNA demethylation promotes flowering and causes partial recovery of the normal branching phenotype. Co-immunoprecipitation assays suggest that AtMBD9 interacts *in vivo* with some regions of the *FLC* gene and binds to histone 4 (H4). Gene expression profile analysis revealed earlier up-regulation of some flower-specific transcriptional factors and alteration of potential hormonal and signal transducer axillary branching regulatory genes. In accordance with this result, AtMBD9 itself was found to be localized in the nucleus and expressed in the flower and axillary buds. Together, these results suggest that AtMBD9 controls flowering time and axillary branching by modulating gene expression through DNA methylation and histone acetylation, and reveal another component of the epigenetic mechanism controlling gene expression.

Keywords: AtMBD9, methylation, acetylation, epigenetics, Arabidopsis, histone.

INTRODUCTION

Epigenetic regulation in eukaryotic cells is performed by a complex array of signaling connections among small RNA species and also by chromatin remodeling. The latter occurs at two possible levels: DNA methylation and histone modification. DNA methylation occurs on more than 30% of cytosine residues (CpG) in some plants (Gruenbaum *et al.*, 1981) and more than 60% in mammals (Gruenbaum *et al.*, 1981; Razin *et al.*, 1984). Specific amino acid residues of histones, usually lysines within the N-terminal tail, are often subjected to a number of covalent post-translational modifications, including acetylation, ADP-ribosylation, methylation, phosphorylation or ubiquitination (Wolffe and Hayes, 1999).

Over the last few decades, a number of lines of evidence have led to the suggestion that CpG methylation in eukaryotes is correlated with gene silencing. Recently, methylation of certain arginines in histones has been shown to regulate flowering time in Arabidopsis (Niu *et al.*, 2007; Schmitz *et al.*, 2008). However, specific histone modifications have different effects on gene expression. For example, acetylation of histone H3 and H4 (He *et al.*, 2003; Peng *et al.*, 2006) and methylation of histone H3 K4 (He *et al.*, 2004) and H3 K36 (Zhao *et al.*, 2005) are associated with activation of FLOWERING LOCUS C (*FLC*), a gene encoding a transcription factor that controls flowering time in Arabidopsis (Michaels and Amasino, 1999; Sheldon *et al.*, 1999). In contrast, methylation of H3 K9 and H3 K27 (Bastow *et al.*, 2004) is associated with *FLC* repression. In addition, there is a strong functional correlation between histone modifications and cytosine DNA methylation (Tariq and Paszkowski, 2004; Mathieu *et al.*, 2007). Some chromatin modifiers such as KRYPTONITE, an H3K9-specific histone methyltransferase, regulate DNA methylation in order to enhance

5-methylcytosines binding at particular regions of DNA and subsequently allow interaction with specific histone residues within the chromatin (Jackson *et al.*, 2002, 2004). The protein structure that binds to the methylated CpG dinucleotide is called the methyl-CpG binding domain (MBD).

Chromatin modifiers often form protein complexes with MBD proteins. Such a situation has been found in mammalian cells, in which MeCP1, a histone deacetylation complex, includes the MBD2 protein (Feng and Zhang, 2001). In Arabidopsis, the DECREASE IN DNA METHYLATION 1 (DDM1) protein co-localized *in vivo* and bound *in vitro* to AtMBD5–7 proteins (Zemach *et al.*, 2005). Likewise, the AtMBD7 protein also interacts with arginine methyltransferase (PRMT11) (Scebba *et al.*, 2007). Twelve putative MBD genes (*AtMBD1–AtMBD12*) have been identified in the Arabidopsis genome (Berg *et al.*, 2003; Springer and Kaeppler, 2005). Six MBD proteins (AtMBD1, 2, 4, 5, 6 and 7) showed specific binding capacity for the methylated CpG sequence *in vitro*. These proteins did not show DNA demethylase activity; however, AtMBD6 demonstrated histone deacetylation activity when a plant extract was treated with the recombinant protein (Zemach and Grafi, 2003).

Loss-of-function analysis of *AtMBD9* mutant lines (*atmbd9-1* to *atmbd9-3*) showed early flowering, increased axillary shoot branches, short plants (Peng *et al.*, 2006), pale leaves and low-seed-yield phenotypes. Early flowering in these lines is due to the down-regulation of *FLC*, which is caused by reduced H3 and H4 acetylation levels at some regions of that locus. The mechanism by which AtMBD9 triggers a reduction in acetylation at *FLC*, and the molecular explanation for the other phenotypic defects, have not yet been determined.

In this study, we aimed to investigate the precise role of AtMBD9 in modulating the flowering and axillary branching phenotypes through biochemical functional characterization of AtMBD9 protein *in vivo* and *in vitro*. We found that AtMBD9 controls gene expression by modifying chromatin structure directly by acetylating histones and indirectly by decreasing the global methylation level of the DNA. Loss of function led to alteration of expression of a number of genes related to flowering and axillary branching pathways in Arabidopsis. AtMBD9 is an example of a transcription factor with two potential epigenetic mechanisms that influence multiple phenotypes.

RESULTS

Over-expression of AtMBD9 cDNA rescues the wild-type phenotype in the atmbd9 mutant

AtMBD9 was originally identified in a reverse-genetic screen in which the mutants showed early flowering and multiple axillary branch phenotypes (Peng *et al.*, 2006). To further confirm the direct influence of *AtMBD9* on these phenotypes, the *AtMBD9* cDNA sequence was initially cloned under the control of the constitutive CaMV 35S promoter (P35S) in the pEGAD vector. After transformation into *atmbd9* and wild-type lines, the transgenic plants were unhealthy and showed a high level of mortality after germination. As it was not possible to obtain a genetically stable homozygous *AtMBD9* transformant line using this strategy, the 35S promoter was replaced by 2023 bp of the *AtMBD9* native 5′ upstream regulatory sequence (P2000). Some transgenic lines obtained using this strategy were healthy and genetically stable for three generations when transformed into either *atmbd9* or wild-type plants. The *atmbd9* lines transformed with this construct flowered almost simultaneously with wild-type plants, and had a similar number of axillary branches. Wild-type Arabidopsis plants transformed with the same construct showed fewer axillary branches and earlier senescence than did untransformed plants, with some of these transgenic lines having only the bolting stem. These results support the view that expression levels of *AtMBD9* affects these traits, with over-expression leading to the opposite phenotype to that which occurred in the mutant lines. The plants transformed with 35S–AtMBD9 showed a higher level of *AtMBD9* expression than wild-type and those transformed with P2000–AtMBD9. However, the expression did not reach wild-type levels when *atmbd9* was transformed with P2000–AtMBD9 (Figure 1). The early flowering phenotype correlated with a low expression level of *FLC* in the *atmbd9* lines. Accordingly, transgenic P2000–AtMBD9 and 35S–AtMBD9 plants restored *FLC* expression to the wild-type level (Figure 1). In the fourth generation of either wild-type or *atmbd9* plants transformed with the P2000–AtMBD9 construct, the phenotype of the homozygous lines started to segregate, and this was due to silencing in the transgene. This situation was noticed in four transgenic lines.

The DNA methylation level modulates the phenotype in the atmbd9 mutants

FLC expression is lower in the *atmbd9* lines and is correlated with a lower acetylation level at the *FLC* locus than is present in wild-type plants. However, it is important also to analyze the *in vivo* DNA methylation pattern at this locus. Therefore, the DNA cytosine methylation within the 867 bp upstream of the start codon, in exon 1 and in only the 358 bp intron 1

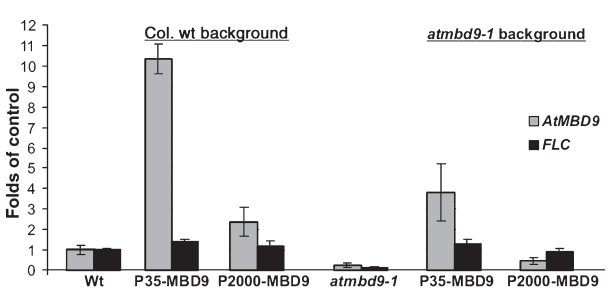

Figure 1. Over-expression of *AtMBD9* cDNA in various Arabidopsis lines.
Quantitative RT-PCR analysis of *AtMBD9* and *FLC* expression in various *atmbd9-1* mutant, wild-type and *AtMBD9* transgenic lines. Expression of Actin-8 was used as an internal control. Bars represent mean ± SD (n = 3).

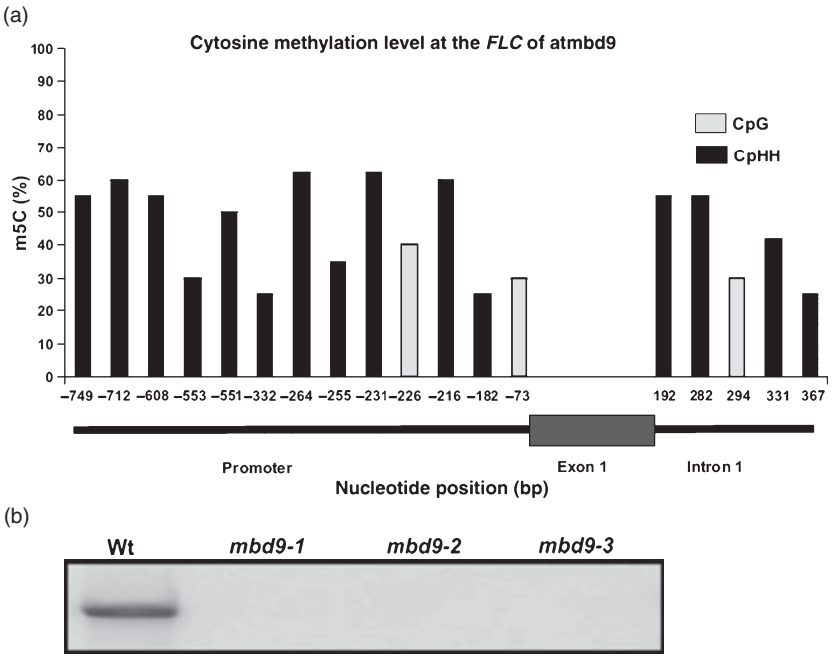

Figure 2. Methylated cytosines within the *FLC* of *atmbd9* mutant lines.
Significant DNA methylation in the promoter and the first intron of *FLC* in the *atmbd9* mutants was detected by sodium bisulfite sequencing.
(a) Distribution and frequency of methylated cytosines (m^5C) calculated based on the bisulfite sequencing results for at least 20 clones.
(b) The DNA methylation was verified by digestion of genomic DNA using the C^mpG-sensitive *Mcr*BC enzyme, followed by PCR amplification using specific primers. Col wild-type genomic DNA was used as a control. Failure to amplify a product after digestion by McrBC indicates that the *FLC* gene is methylated in the *atmbd9* lines.

of the *FLC* gene was analyzed using the sodium bisulfite DNA sequencing technique. The results revealed the presence of 18 methylated cytosine sites within the *FLC* promoter, exon 1 and intron 1 sequences in the *atmbd9* lines. These methylated cytosine sites were not found in the Col wild-type counterparts (Figure 2a). Fifteen of these sites showed the CpHH motif (where H is A, C or T) and three the CpG motif. Methylation was verified by using PCR to amplify the genomic DNA after digestion with *Mcr*BC endonuclease, which cleaves DNA containing methylcytosine (Figure 2b), and also by using a methylation-sensitive restriction enzyme coupled with Southern blot analysis (Figure S1). To whether the increase in cytosine methylation level occurred globally across the genome, and also to investigate the direct influence of *AtMBD9* over-expression on the DNA methylation level, global DNA methylation analysis was carried out using an ELISA-like reaction and *atmbd9*, wild-type, P2000–AtMBD9/*atmbd9-1* and P2000–AtMBD9/WT transgenic DNA. The *atmbd9* genomic DNA was found to have approximately 15% more methylation than the Col wild-type Arabidopsis plants (Figure 3). This result was verified by the use of methylation-sensitive restriction enzymes coupled with Southern blot analysis (Figure S2). In contrast, the percentage of methylated cytosine was similar to the wild-type level in the transgenic P2000–AtMBD9/*atmbd9-1* line, and the P2000–AtMBD9/WT DNA had a slightly lower level of methylated cytosine residues (Figure 3). Therefore, AtMBD9 clearly helps regulate the global level of cytosine methylation.

To investigate the effect of cytosine methylation on flowering time and the axillary branching habit in *atmbd9*

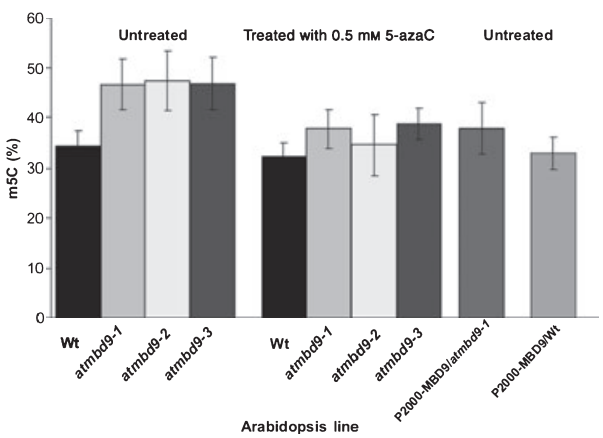

Figure 3. Treatment effect of 0.5 mM 5-azaC on the global genomic DNA methylation level in various Arabidopsis lines. Values are means ± SD of three replicates.

and Arabidopsis wild-type, DNA methylation levels were transiently reduced by treating the plants at an early stage with the cytosine methyl transferase inhibitor 5-azacytidine (5-azaC) (Jones, 1985; Haaf, 1995). After treating the seedlings with 0.5 mM 5-azaC for 5 days, growth of all plants slowed down by 1 week, and the differences in flowering time and axillary branching number between wild-type and *atmbd9* were significantly reduced (Table 1 and Figure 4a,b). In addition, there was partial recovery of *FLC* expression after treatment with 0.5 mM 5-azaC (Figure 4c) because of the partial reduction in DNA methylation (Figure 4d). Therefore, the global DNA methylation

Treatment	Col wild-type	*atmbd9-1*	*atmbd9-2*	*atmbd9-3*
0.0 mM	27.8 ± 0.7 (18)	21.5 ± 1.3 (18)	21.7 ± 1.3 (18)	21.1 ± 0.8 (18)
	3.6 ± 0.6	5.1 ± 1.0	5.4 ± 0.8	5.2 ± 1.1
0.3 mM	34.4 ± 1.4 (10)	30.8 ± 1.4 (10)	31.2 ± 1.9 (4)	30 ± 2.1 (10)
	2.9 ± 0.7	3.7 ± 0.9	4 ± 0.8	3.8 ± 0.8
0.5 mM	35.1 ± 0.8 (13)	33.2 ± 0.8 (5)	33.5 ± 1.7 (10)	34.4 ± 1.1 (11)
	3.1 ± 0.5	3.4 ± 0.5	3.1 ± 0.7	3.3 ± 0.5
1 mM	34.2 ± 2.1 (15)	29.9 ± 2.1 (18)	29.7 ± 1.2 (10)	28.8 ± 1.2 (8)
	2.9 ± 0.7	3.5 ± 1.4	3.7 ± 1.5	3.8 ± 1.4

Table 1 The effect of 5-azaC treatment on the flowering time (upper row) and the axillary branching number (lower row) in Arabidopsis

Results are shown as mean ± SD. The numbers of plants tested for each treatment are shown in parentheses.

level of the treated plants was reduced, and changed the flowering time and shoot branching pattern in the *atmbd9* lines such that it was closer to that seen in wild-type plants.

AtMBD9 acetylates histones but does not demethylate C^mpG sites *in vitro*

Recombinant full-length AtMBD9 was expressed and purified from insect cells and used for various biochemical assays. In addition, specific polyclonal antibodies against AtMBD9 were raised in rabbits, and used in some of these assays (Figure S3). Loss of function of *AtMBD9* leads to an increase in the DNA methylation level. In addition, this level was decreased in the *atmbd9*-complemented transgenic lines (Figure 3). In view of this result, a DNA demethylation assay based on methylation endonuclease sensitivity was performed using the recombinant AtMBD9 protein. Unexpectedly, the recombinant AtMBD9 did not show any detectable DNA demethylation activity when an *in vitro*-methylated *FLC* DNA sequence was used as the substrate (Figure S4), but did show significant acetylation activity *in vitro*. The acetylation activity was measured at various time points using various amounts of recombinant protein. The increase in activity was found to be directly correlated to the amount of recombinant protein used in the reaction (Figure 5a). The acetylation activity was confirmed using the gel-based method described by Brownell *et al.* (1999) (Figure 5b).

The acetylation levels of histones H3 and H4 in the *atmbd9* and wild-type were measured *in vivo* using an immunoblotting technique. In agreement with the *in vitro* enzymatic assay, histone H3 and H4 extracted from the wild-type have a higher acetylation level than those extracted from the *atmbd9* mutant. The acetylation level was even higher in the over-expressed P2000–AtMBD/WT lines (Figure 5c). In addition, histone H4 was detected in the AtMBD9 immunoprecipitated complex when it was probed using acetylation-specific H4 antibodies in the Western blot (Figure 5d,e). Histone H3 was not detected in the same complex, which may reflect specificity and a direct functional interaction between H4 and AtMBD9.

ChIP assay reveals a direct interaction between AtMBD9 and FLC

It has been shown that the *FLC* expression level is regulated by various transcription factors and also by environmental conditions such as light and temperature (Mouradov *et al.*, 2002). Peng *et al.* (2006) previously reported that loss of *AtMBD9* function inhibits *FLC* expression by reducing the acetylation level in some regions within this locus. By using AtMBD9-specific antibodies in a chromatin immunoprecipitation (ChIP) assay, we found that AtMBD9 binds to three regions of *FLC* (B, D and I) previously defined by Bastow *et al.* (2004) and Peng *et al.* (2006) (Figure 6). Regions B and D span part of the promoter and the first exon, and part of the first intron of *FLC*, respectively, and region I covers the junction region of intron 6 and exon 7. Compared with the other regions, the highest degree of interaction was found in region I (Figure 6f).

Sodium bisulfite sequence analysis of *FLC* region B in the *atmbd9* mutant revealed the presence of two methylated CpG sites and several CHH sites (where H is A, C or T) within this region (Figure 2). These methylated cytosines probably represent AtMBD9 binding sites in wild-type chromatin. The binding may be followed by demethylation of these cytosines by another protein, which does not occur in the absence of AtMBD9.

AtMBD9 is localized in the nucleus

AtMBD9 contains two nuclear localization signals (NLS) that reside within the N-terminal and centric domains of the protein. The PKRRKTS and KLVRRRK amino acid NLS motifs start at the 335 and 1348 amino acids of AtMBD9, respectively (Figure S3). Full-length AtMBD9 fused with GFP showed cytoplasmic aggregations and did not localize to a specific cellular compartment when transiently expressed in either Arabidopsis cells, B21 tobacco suspension cells or onion epidermal cells. This might be due to the large size of the GFP–AtMBD9 fusion protein. Therefore, the parts of the AtMBD9 that include the NLSs were separately fused with GFP and used for the locali-

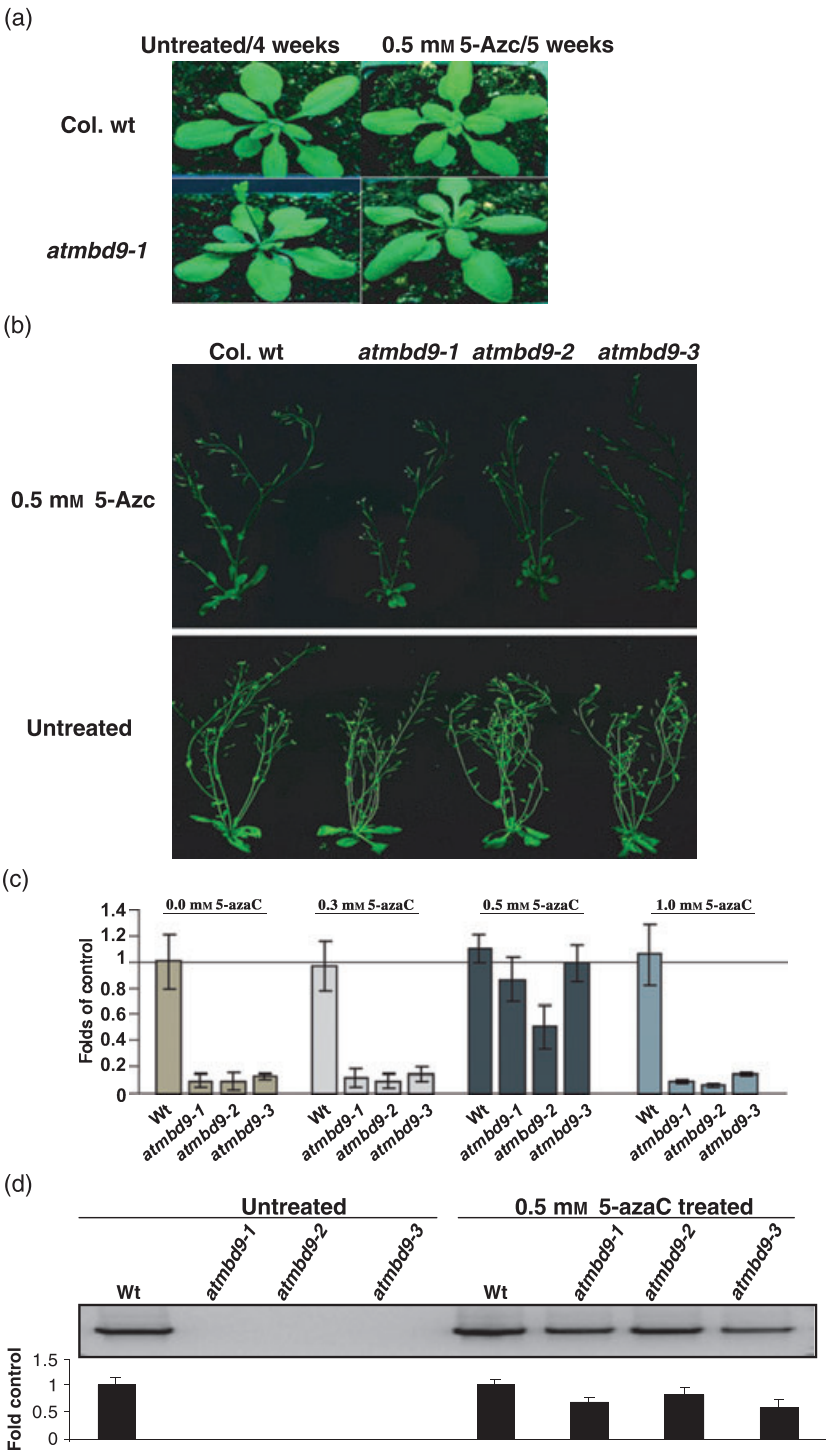

Figure 4. Effect of 5-azaC on the Arabidopsis phenotypes, *FLC* expression and DNA methylation.
(a) *atmbd9-1* seedlings treated with 5-azaC show a wild-type flowering time.
(b) Recovery of the number of wild-type axillary branches in *atmbd9-1* after 5-azaC treatment.
(c) Quantitative RT-PCR analysis of FLC expression in *atmbd9* mutants and Col treated with 5-azaC. Expression of Actin-8 was used as an internal control. Bars represent mean ± SD ($n = 3$).
(d) The DNA methylation status of the 5-azaC-treated plants was verified by digestion of genomic DNA using $C^{m}pG$-sensitive *Mcr*BC enzyme, followed by PCR amplification using specific primers. Col wild-type and the untreated *atmbd9* genomic DNA were used as a control. Partial recovery of the PCR amplification after digestion with *Mcr*BC indicates that the *FLC* gene is less methylated in the 5-azaC-treated *atmbd9* mutant lines.
(e) Band intensity was quantified, and the mean fold changes (±SD) of three experiments are shown.

zation studies. The results showed that the peptides containing the N-terminal and the centric NLSs are both able to direct the GFP to the nucleus of onion epidermal cells (Figure 7). This result provides direct evidence that AtMBD9 is a nuclear protein and contains two functional NLSs.

AtMBD9 is expressed in the shoot apical region and shoot branching sites

As AtMBD9 regulates *FLC* transcription and shoot branching in Arabidopsis, it is informative to investigate the spatial and temporal expression pattern of *AtMBD9*, and compare the

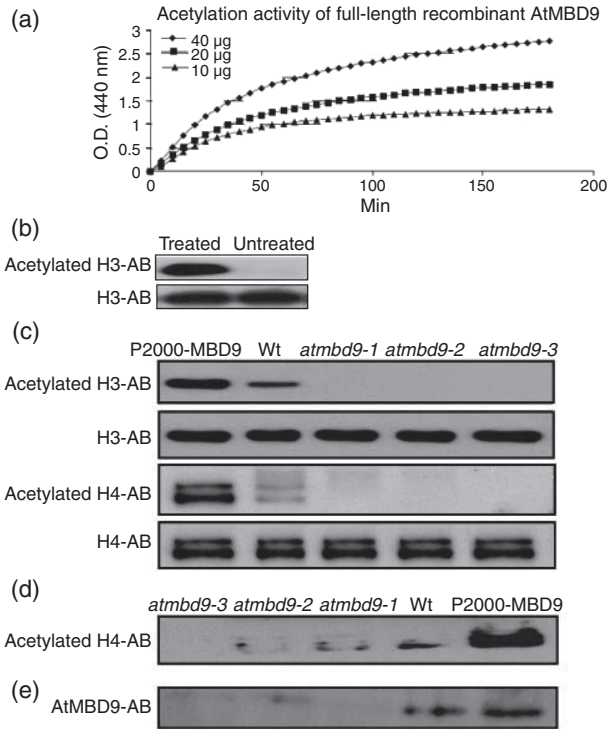

Figure 5. *In vitro* and *in vivo* acetylation activity of AtMBD9.
(a) Histone acetylation (HAT) activity of various amounts of recombinant full-length AtMBD9. The mean of three readings each for three samples was taken at various time points for each sample.
(b) Recombinant histone H3 was treated *in vitro* with recombinant AtMBD9 protein, and the HAT activity was detected by Western blotting using acetylated H3 antibodies (H3-AB).
(c) Endogenous histone H3 and H4 acetylation levels for various Arabidopsis lines were measured by immunoblotting reaction with specific antibodies (AB). Antibodies against histones H3 (H3-AB) and H4 (H4-AB) were used as a protein loading control.
(d) *In vivo* interaction of AtMBD9 with acetylated histone H4. The interactions were detected using specific antibodies (H4-AB). The two bands in the Western blot represent the two acetylation forms of H4.
(e) Immunoprecipitation of AtMBD9 using acetylated H4 antibodies. The interactions were detected using specific AtMBD9 antibodies (AtMBD9-AB).

resulting information with the expression pattern of *FLC* and the occurrence of shoot branching. Using RT-PCR, Berg *et al.* (2003) demonstrated that *AtMBD9* is expressed in the rosette leaves, flowers and stems, but no *AtMBD9* transcript was detected in the root, green siliques and seeds. To examine *AtMBD9* expression in more detail throughout Arabidopsis development, we fused the *AtMBD9* promoter (PAtMBD9) with the GUS reporter gene, and transformed this construct into Arabidopsis plants. Expression of the GUS gene under the control of the *AtMBD9* promoter was detected at various developmental stages by histochemical staining with 5-bromo-4-chloro-3-indolyl-β-D-glucuronic acid (X-Gluc).

At 7 days after germination, *AtMBD9* expression was detected in the vascular system of the cotyledons and hypocotyls, but not in root tissue. The strongest GUS staining was found in the shoot apical region (Figure 8a) where dividing cells reside and *FLC* shows the highest expression (Michaels and Amasino, 2001). After further growth of the Arabidopsis plants, *AtMBD9* was expressed in the vascular tissues of rosette leaves, old inflorescence stems and cauline leaves (Figure 8b–d). High expression of *AtMBD9* was always detected in rosette regions where secondary rosette branches are produced (Figure 8b), and at inflorescence junctions where the outgrowth of tertiary branches occurs (Figure 8c). This pattern fits well with the fact that *AtMBD9* regulates the Arabidopsis shoot branching trait. In addition, 14-day-old plants showed strong PAtMBD9–GUS activity in root junction parts where lateral roots are formed (Figure 8b). In flowers, PAtMBD9–GUS staining was visible only in the vascular tissues of sepals, the filament and the receptacles (Figure 8e). In green siliques, *AtMBD9* was expressed only at the junctions between siliques and pedicels (Figure 8f).

Transcriptome profiling of atmbd9-1 revealed the molecular events associated with the phenotypic variation

There is an increase in overall DNA methylation in the *atmbd9* mutant, and one would expect this to have a significant affect on the transcriptome. Therefore, a set of whole-genome microarray experiments were performed on apical bud tissue isolated from the first-producing rosette leaves and buds of *atmbd9-1* and wild-type plants. Bud tissue was chosen in the expectation that this would help explain differences in the axillary branching phenotype. The microarray results showed that there are 333 genes whose expression is significantly different in the *atmbd9* mutant, with 158 and 175 genes up- and down-regulated, respectively. These genes were classified based on their biological functions in the plant (Table S1 and Figure S5). The expression level of 21 representative genes was confirmed using RT-PCR (Figure S6). Proportionately there are more up-regulated genes encode proteins that are localized in the nucleus and associated with transcription factor activity or DNA/RNA binding and involved in developmental processes compared to those that are down-regulated.

The expression profile contains genes with both direct and indirect relationships to flowering, branching and hormonal metabolic pathways. For example, transcriptional factors associated with flower initiation and developmental pathways, such as *SEPALLATA 1* and *3* (*SEP1* and *SEP3*) and *SQUAMOSA promoter binding protein-like 3* and *4* (*SPL3* and *SPL4*) were prematurely expressed at a high level in the *atmbd9* mutant (Table S1), indicating their involvement in the early flowering phenotype in *atmbd9-1*. It is well-demonstrated that hormonal balance plays an important role in flowering and branching in plants. Therefore, it is not surprising that hormone-related genes such as *ETHYLENE-INSENSITIVE3*, *EIN3/EBF2-BINDING F BOX PROTEIN 2*

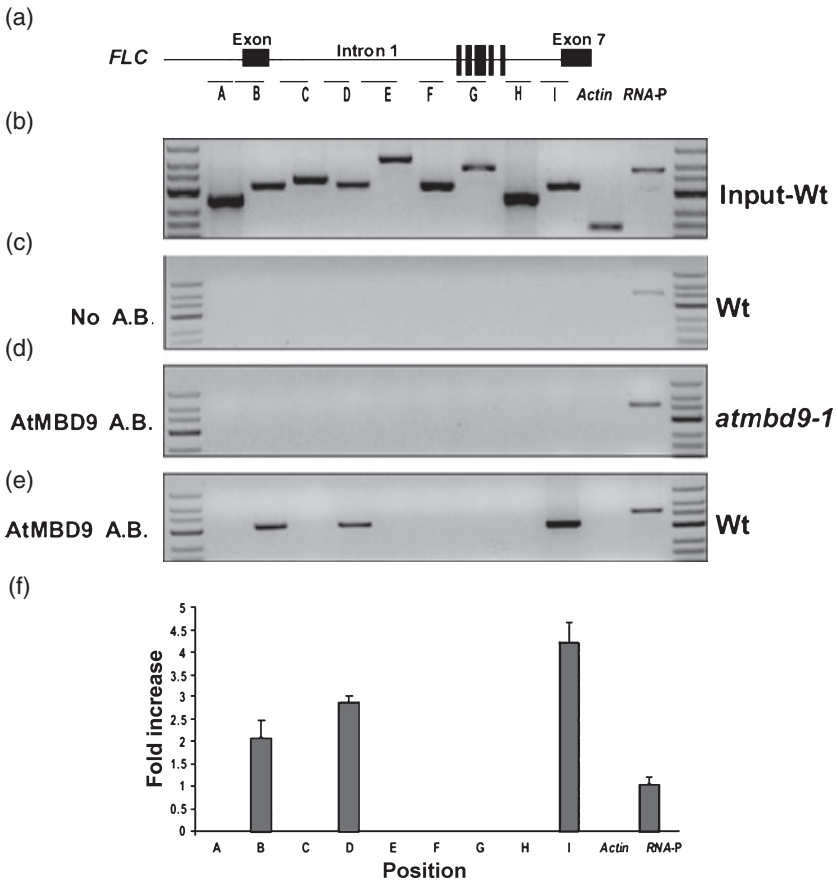

Figure 6. Chromatin immunoprecipitation assays (ChIP) in wild-type and *atmbd9-1* Arabidopsis.
(a) The genomic structure of *FLC* and the regions tested in the ChIP assay. Coding regions are indicated by black boxes.
(b) PCR products of input DNA from the wild-type used in the ChIP assay.
(c) Control ChIP assay using chromatins extracted from wild-type plants and without using AtMBD9 antibodies.
(d) Control ChIP assay using chromatins extracted from *atmbd9-1* and AtMBD9 antibodies.
(e) ChIP assay performed using chromatins extracted from wild-type Arabidopsis and the AtMBD9 antibodies.
(f) Signal intensities were normalized relative to RNA polymerase 2 ChiP control reactions (RNA-P), and the mean fold changes (±SD) of three experiments are shown. Actin-2/7 was used as a PCR-negative control for the ChIP assays.

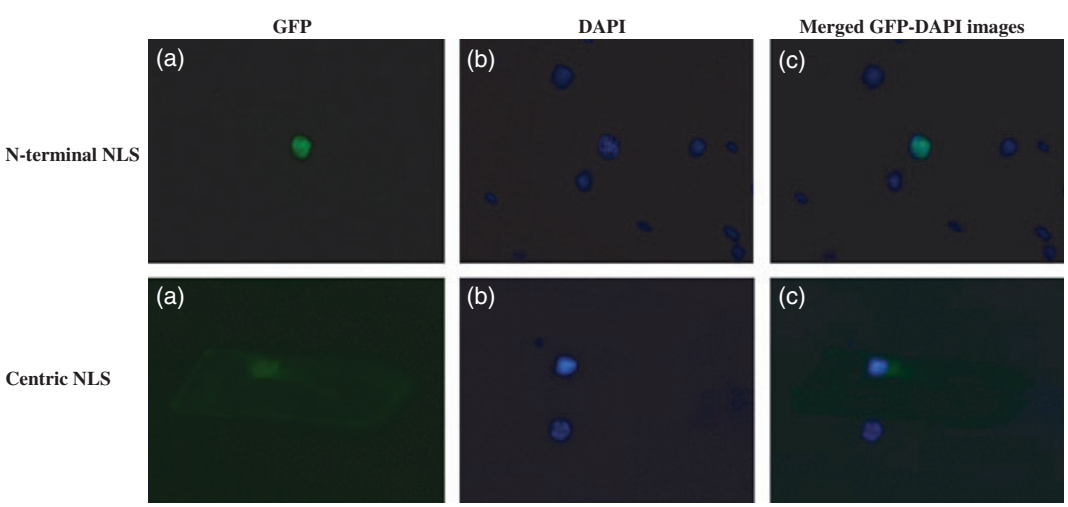

Figure 7. Subcellular localization of AtMBD9.
(a) GFP fused with NLS expressed in the nucleus of onion epidermal cells.
(b) Nucleus of onion epidermal cells stained with 4′-6-Diamidino-2-phenylindole (DAPI).
(c) Merged image of (a) and (b).

(At5g25350), ETHYLENE RECEPTOR SUBFAMILY 1 (*ERS1*), (At2g40940), *GA REQUIRING 4* (*GA4*), the GA-related gene *S-ADENOSYLMETHIONINE-DEPENDENT METHYLTRANSFERASE/GIBBERELLIN CARBOXYL*-O-*METHYLTRANSFERASE* (*GAMT2*) and the gene encoding cytochrome P_{450} (CYP79B2, At4g39950) were differentially expressed in the *atmdb9* mutant (Table S1). This latter gene encodes a protein that converts tryptophan to indo-3-acetaldoxime

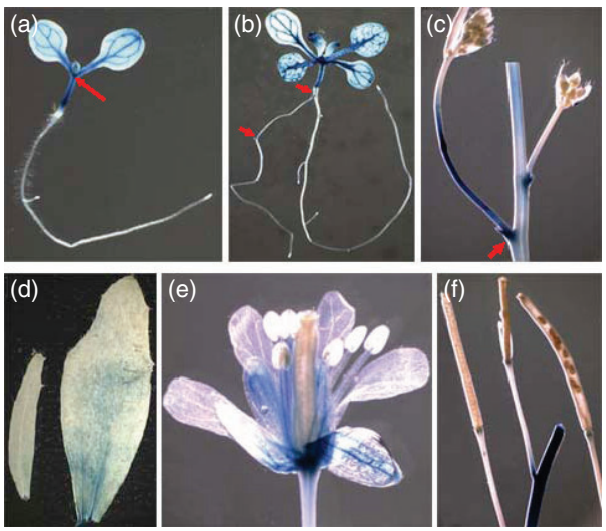

Figure 8. Localization of PAtMBD9-GUS expression in Arabidopsis plants.
(a, b) Detection of PAtMBD9-GUS activity in 7- and 14-day-old plants, respectively, showing strongest GUS staining in the shoot apex and rosette region.
(c) High PAtMBD9-GUS activity in old inflorescences and the junctions at which lateral inflorescences are produced.
(d) PAtMBD9-GUS staining in old cauline leaves.
(e, f) Analysis of PAtMBD9-GUS activity in flower (e) and siliques (f).

(IAOx), a precursor that is required for IAA and indole glucosinolate biosynthesis (Hull *et al.*, 2000).

In addition, genes involved in signal transduction pathways that lead to multiple axillary branches were differentially expressed in the *atmbd9* mutant. These include the plasma membrane intrinsic protein subfamily *PIP2* (At2g37170) and the leucine-rich kinase protein (At5g25930), which are involved in the inositol phosphate metabolism pathway, and SETH2 (At3g45100) (Gillmor *et al.*, 2005), which is involved in the first step of the glycosylphosphatidylinositol-anchored biosynthesis pathway.

The genomic DNA of *atmbd9* is hypermethylated. Coincidentally, *atmbd9-1* showed expression alteration of some genes encoding putative nucleic acid methyl transferases and binding proteins, including up-regulation of methyltransferase type 11 (At3g01660), the jmjC domain-containing protein At3g20810, and ribosomal RNA RrmJ/FtsJ-like methyltransferase (At5g13830), and down-regulation of the methylcytosine-binding protein, VARIANT IN METHYLATION 4 (VIM4) (At1g66040) (Woo *et al.*, 2007).

DISCUSSION

AtMBD9 expression is critical for normal growth and development

AtMBD9 controls gene expression directly through histone acetylation and indirectly through DNA methylation. It was previously shown that mutants in this gene had altered developmental patterns, particularly with regard to flowering time and shoot branching (Peng *et al.*, 2006). In the present study, over-expression of *AtMBD-9* under the control of the CaMV 35S promoter generally caused plant death at an early stage, and those plants that did survive were genetically unstable. When expression was regulated by the native promoter, the resulting construct was able to rescue most of the phenotypes of the mutant gene. However, these plants eventually showed genetic instability as well. Therefore, tight control of *AtMBD9* gene expression is important for normal growth and development.

When the *AtMBD9* promoter sequence was fused to the GUS reporter gene, *AtMBD9* was found to be highly expressed in the shoot apical region and the transition zone where transition from shoot meristem to floral meristem occurs (Figure 8a). High expression of *AtMBD9* was also detected in the regions where lateral shoot branches (inflorescences) are produced (Figure 8b,c). The phenotypic alteration associated with *AtMBD9* mutations, and the expression pattern seen in these experiments during growth and development, reflect the biological function of this protein in flowering and axillary branching in Arabidopsis.

Increased DNA methylation is associated with the *atmbd9* mutant phenotypes

The molecular events associated with the loss of function of *AtMBD9* in Arabidopsis provide an important indication of its role in the regulation of gene expression. In these mutants, there is lower expression of the flower repressor gene *FLC* due to low histone acetylation (Peng *et al.*, 2006) and a high DNA methylation level (Figure 2) at this locus. The normal time of flowering was restored in *atmbd9* mutants either after treatment with 5-azaC or complementary genetic transformation. These both led to a corresponding increase in *FLC* expression. In addition, both 5-azaC and complementation of the *atmbd9* mutation led to partial recovery of the wild-type branching pattern, although the target genes involved in this process are still not known.

Mutations within *DECREASE IN DNA METHYLATION1* and *2* (*DDM1* and *DDM2*), *DNA METHYLTRANSFERASE1* (*MET1*) (Vongs *et al.*, 1993; Kakutani *et al.*, 1996), and the DNA demethylase gene, *REPRESSOR OF SILENCING GENES1* (*ROS1*) (Agius *et al.*, 2006) altered the overall level of cytosine methylation and caused various developmental defects in Arabidopsis. This effect on DNA methylation level led to different effects on flowering time depending on the Arabidopsis ecotypes studied. DNA hypomethylation in *ddm1* and *met1-1* mutations caused late flowering in Columbia and Landsberg *erecta* (Kakutani, 1997; Kankel *et al.*, 2003), but hypomethylation induced by vernalization or 5-azaC treatment promoted flowering in the vernalization-responsive Arabidopsis ecotype C24 (Burn *et al.*, 1993; Finnegan *et al.*, 1998). However, in both cases, the *FLC* expression level was critical for determining flowering time,

but these studies did not indicate whether the DNA methylation status of the *FLC* had been changed. However, in our study, we found that down-regulation of FLC in the early flowering *atmbd9* mutant was directly due to methylation in the DNA sequence (Figure 2) and reduction of the acetylation levels (Peng *et al.*, 2006).

As inactivation of AtMBD9 causes DNA hypermethylation in Arabidopsis, DNA demethylation activity was one of the putative functions of AtMBD9 that we investigated in this study. However, the full-length recombinant AtMBD9 protein produced in insect cells did not show any DNA demethylase activity when assayed *in vitro*. Although the possibility that multiple protein complexes are required for the AtMBD9 DNA demethylation activity cannot be ruled out, based on the *in vitro* assay, the simplest explanation is that the methylation status of the genomic DNA is influenced indirectly by *AtMBD9*. Transcription profile analysis of *atmbd9-1* revealed expression alterations in four nucleic acid methyltransferase genes (*METHYLTRANSFERASE* type 11, *RRMJ/FTSJ-LIKE METHYLTRANSFERASE*, *jmjC* domain-containing protein, and *VIM4*) (Table S1). These changes in gene expression may have an impact on the DNA methylation status in the *atmbd9* mutant lines.

AtMBD9 modulates gene expression directly through histone acetylation

In order to determine the specific biochemical function of AtMBD9 in controlling gene expression, the recombinant protein was tested for histone acetylation, deacetylation and some potential histone methyltransferase activities. Enzymatic activity assays showed that full-length recombinant AtMBD9 catalyzes the acetylation reaction *in vitro* (Figure 5a,b). *AtMBD9* does not code for a well-defined histone acetyl transferase catalytic domain. Thus, there must be a novel histone acetyl transferase domain within AtMBD9 given the *in vitro* acetylation activity and the presence of a BROMO/Bah domain as is usually found in other histone acetylation proteins (Dhalluin *et al.*, 1999; Goodwin and Nicolas, 2001; Hassan *et al.*, 2006).

In agreement with the enzymatic function *in vitro*, mutant lines lacking AtMBD9 activity showed significantly lower overall histone H3 and H4 acetylation levels than did wild-type Arabidopsis (Figure 5c). Results obtained from immunoprecipitation of the total histones suggest that AtMBD9 also binds to acetylated H4 histones (Figure 5d). The reduction in acetylation level in the *atmbd9* lines was previously observed by Peng *et al.* (2006), who immunoprecipitated *FLC* chromatin using acetylated histone H3 and H4 specific antibodies in a ChIP assay.

AtMBD9 binds *in vivo* to several *FLC* chromatin regions covering part of the promoter and transcription initiation site (region B), the first exon (region D) and a sequence within intron 6 and exon 7 (region I) (Figure 6). It has been reported that chromatin in these regions is subjected to several histone alterations leading to regulation of *FLC* expression. For example, the *FLC* region B overlaps with a low acetylated H3 region upstream of the transcriptional start site in Arabidopsis after vernalization (Sung and Amasino, 2004). In addition, mutations in the flowering time locus of the autonomous pathway (FVE) led to an increase in acetylation in region D of *FLC* in earlier-flowering plants (Ausin *et al.*, 2004). The AtMBD9 ChIP library was highly enriched with the *FLC* sequence that covers the junction between intron 6 and exon 7 (region I). This region was found to interact with FLOWERING LOCUS D (FLD), LYSINE-SPECIFIC DEMETHYLASE 1 and the RNA-binding protein FCA that together mediate H3K4 demethylation in *FLC* (Liu *et al.*, 2007). Together, these results confirm that AtMBD9 binds to DNA and histones, and therefore can modulate key regulatory regions across the *FLC* chromatin by increasing their acetylation level and consequently enhancing *FLC* gene expression. The chromatin regions B and D of *FLC* that bind to AtMBD9 closely flank region C, which has a low histone H4 acetylation level in *FLC* of *atmbd9* mutants, as previously determined by Peng *et al.* (2006). The variations between the two ChIP assays could be due to a difference between the AtMBD9 DNA binding and histone acetylation active sites on the compact nucleosomal structures, or due to different interaction and detection capacities between AtMBD9 and the acetylated histone H3 and H4 antibodies used in the assays.

AtMBD9 controls flowering time and lateral branch formation through a novel epigenetic mechanism

AtMBD9 encodes a protein containing a number of domains that are predicted to have activities involved in the epigenetic control of gene expression through chromatin modifications such as histone acetylation and methylation, and the 5-methylcytosine (m^5C) binding domain that allows binding to DNA. It has been previously reported that methylated DNA and histone modification have integral and overlapping roles in epigenetic regulation in plants (Tariq and Paszkowski, 2004; Vaillant and Paszkowski, 2007; Saze *et al.*, 2008; Zhang *et al.*, 2008) as well as in mammals (Allen and Antoniou, 2007; Sridhar *et al.*, 2007; Vincent *et al.*, 2007). AtMBD9 affects both on the DNA methylation and *in vitro* histone acetylation activity, and provides a direct link between DNA methylation and histone alterations. These features functionally distinguish AtMBD9 from other MBD proteins.

The mechanism by which AtMBD9 interacts with chromatin is not completely understood. However, based on our findings, we propose the following model for its action (Figure 9): (i) AtMBD9 binds to chromatin via methylated DNA and then to histone H4, (ii) this binding leads to acetylation of the histones, and (iii) this leads to demethylation of DNA by another protein. A similar mechanistic link between histone acetylation and DNA demethylation has

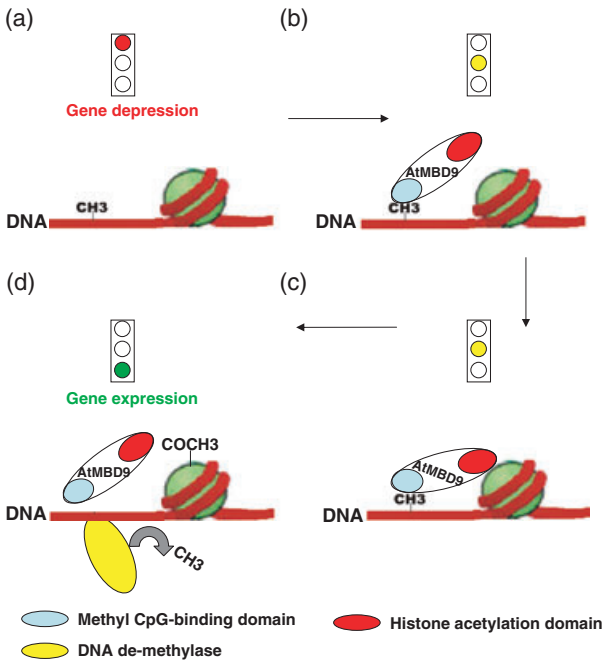

Figure 9. Proposed mechanism for gene expression controlled by AtMBD9. The traffic light signal represents the gene expression status in each step. The mechanism suggests a DNA- and histone-binding points within a nucleosome.
(a) Inhibition of gene expression due to the presence of a methyl group (CH3) on the DNA.
(b) AtMBD9 binds to both methylated DNA and histone H4.
(c) Meanwhile, DNA demethylase binds to the methyl group of DNA.
(d) Addition of the acetyl group (COCH3) to histone H4 by AtMBD9 and removal of the CH3 group from the DNA by a DNA demethylase enhances gene expression.

been previously suggested to control gene expression in human embryonic kidney (HEK) cells. In this case, DNA demethylation was followed by histone acetylation (D'Alessio *et al.*, 2007). Another pathway was hypothesized to describe the silencing of some tumor suppressor genes in humans (Belinsky *et al.* 2003; Issa, 2004; Brock *et al.*, 2007), in which the MBD protein binds to abnormally methylated CpG and serves as a ligand for the histone deacetylation protein. However, AtMBD9 can be recruited to the CpG sites as well as acetylating histones. In addition to this pathway, it is possible that AtMBD9 enhances DNA methylation by up-regulating some DNA methylation-related genes. The absence of functional AtMBD9 in a cell would thus lead to accumulation of methylated cytosines in the genome and consequently to a significant change in global gene expression.

In conclusion, the *atmbd9* mutation causes changes in flowering time and axillary branching. The AtMBD9 protein has a variety of domains that interact with chromatin, and in this study was found to acetylate histones *in vitro*. In addition, an increase in the global DNA methylation and a reduction in histone acetylation levels were observed in the mutant line, while the lines over-expressing this protein showed the opposite effect. As an example, the *atmbd9* line shows low acetylation in the chromatin regions of the *FLC* gene, and an increase in DNA methylation at some cytosine residues. This explains the changes seen in FLC expression. This information supports the hypothesis that there is a cooperative mechanism between DNA methylation and histone modifications that controls gene expression.

EXPERIMENTAL PROCEDURES

Plant material, growth conditions and treatment with 5-azaC

For 5-azaC treatments, seeds were surface-sterilized, cold treated for 2 days at 4ºC, and germinated for 6 days under the same growth conditions on 1 mm Whatman filter paper saturated with either water or a solution of 0.3, 0.5 or 1 mM 5-azaC (Sigma-Aldrich, http://www.sigmaaldrich.com/). The solutions were prepared freshly every day. After germination, seeds were grown on regular LA4 soil (Sunshine, http://www.sungro.com/index.php) under normal conditions.

Cloning of the AtMBD9 cDNA and plant genetic transformation

Total RNA was extracted from wild-type plant leaves using an RNeasy plant mini kit (Qiagen, http://www.qiagen.com/), and the cDNA was amplified using primer pair F-MBD9 (5′-CTGACCGGTATGGAACCCACTGATTCTACTAACG-3′) and R-MBD9 (5′-CTAGGATCCCTCGGGTTCTTTCCTTTTCTTG-3′). The amplified fragment was digested with *Age*I and *Sma*I, and cloned into the binary pEGAD expression vector after removing the EGFP coding region from the plasmid (Cutler *et al.*, 2000). The resultant construct was named P35S-AtMBD9-pEGAD. Subsequently, the 35S promoter of the P35S-AtMBD9-pEGAD was replaced by putative promoter residues within the 2023 bp upstream of the AtMBD9 coding region. The putative promoter was amplified from the genomic DNA by PCR using primer pair F-Promoter (5′-CCACCCACCGTATCCAATTGCTACTAT-3′) and R-Promoter (5′-GTCTAACCGGTTATTCGATTAGGTTAATGGAATC-3′), digested with *Stu*I and *Age*I, and cloned upstream of *AtMBD9* in the pEGAD vector. The resultant construct was named P2000-AtMBD9-pEGAD. In order to the fuse the *AtMBD9* promoter to the GUS reporter gene, a DNA fragment (1.4 kb) upstream of the *AtMBD9* coding region was amplified from the Arabidopsis genome by PCR using primer pair F-GUSMBD9 (5′-ATCTTCTAGAGTCGTCGTAGTCATACT-3′) and R-GUSMBD9 (5′-ATCTCCATGGAATCGAGCATTGTTTGC-3′). The PCR product was digested with *Xba*I and *Nco*I, and cloned between the *Xba*I and *Nco*I sites of the GUS reporter gene fusion binary vector pCAMBIA3301 (Cambia Institute, http://www.cambia.org). All constructs were amplified in *Escherichia coli* DH10b cells and transformed into *Agrobacterium tumefaciens* EHA105 cells. Wild-type plants and *atmbd9* mutant lines were transformed with P35S-AtMBD9-pEGAD and P2000-AtMBD9-pEGAD using the floral dipping method. Transgenic plants were selected by spraying with BASTA (Glufosinate) herbicide (Bayer Crop Science, http://www.bayercropscience.ca).

For determination of subcellular localization, the *AtMBD9* DNA sequences coding for the N-terminal NLS (562–1587 bp) and the centric NLS (3442–4620 bp) were independently cloned in-frame with the GFP protein under the control of the 35S promoter. The N-terminal NLS cDNA sequence was amplified by PCR using primer pair F-NNLS (5′-CGCGGATCCTATGCAATGATGCATTCAAGC-′3) and

R-NNLS (5′-TGCTCTAGATCAATATATCATCTCCAAGAGGTGGGC-′3), and the centric NLS cDNA sequence was amplified using primer pair F-CNLS (5′-CGCGGATCCGCTGCAGACGAGGATAAAGTC-′3) and R-CNLS (5′-TGCTCTAGATCATATAGGTAGCTCATGCCTCCCAG-G-′3). After digestion with *Bam*HI and *Xba*I, the PCR products were cloned into the pRLT2-GFP plasmid (kindly provided from Dr Robert Mollen at Guelph University) and transformed by particle bombardment into onion epidermal cells.

Peptide antibodies

The DNA sequence (4350–5235 bp) coding for a partial AtMBD9 peptide was amplified by PCR using primer pair F-ProMBD9 (5′-CGTATTCCATATGGAACCGAGTATTCTGAAGGAA-3′) and R-ProMBD9 (5′-CGGGAATTCAGCAGATAAATTCTGAGCTTGTTT-3′). The PCR product and plasmid were digested with *Sal*I and *Sma*I cloned into the pTYB2 vector (New England Biolabs, http://www.neb.com/nebecomm/default.asp). The construct was amplified in *E. coli* DH10B cells and transformed into *E. coli* expression host strain ER2566 cells. The protein was expressed and purified using the IMPACT system (intein-mediated purification with an affinity chitin-binding tag) (New England Biolabs), according to the manufacturer's instructions. The AtMBD9 peptide was used as an antigen to produce polyclonal antibodies in rabbits using the service obtained from Cedarlane (http://www.cedarlanelabs.com), and the antibodies were purified using the method described by Smith and Fisher (1984).

Chromatin immunoprecipitation

Chromatin immunoprecipitation (ChIP) assays were performed as described previously by Johnson and Bresnick (2002). Purified AtMBD9 antibodies were used in the assay to precipitate AtMBD9-associated DNA in the chromatin of wild-type and *atmbd9* leaves. The resultant DNA was used to amplify *FLC* regions using the primer pairs given by Bastow *et al.* (2004) and Peng *et al.* (2006). The amounts of PCR products were quantified using IMAGEJ software (Abramoff *et al.*, 2004).

Protein immmunoprecipitation and immunoblotting

Total proteins were extracted from leaves of Arabidopsis seedling lines grown on MS medium for 10 days. The leaves were harvested, ground in liquid nitrogen and extracted using 50 mM Tris, pH 7.5, 150 mM NaCl, 1 mM EDTA, 0.1% v/v Triton X-100, 0.2 mM phenylmethylsulfonyl fluoride (PMSF) and complete protease inhibitor cocktail tablets (Roche Applied Science, http://www.roche.com). AtMBD9 and associated proteins were precipitated from the total protein extract using Dynabeads Protein G (Invitrogen, http://www.invitrogen.com/) and either the purified AtMBD9 antibody or anti-acetyl-histone H3 or H4 antibodies according to the manufacturer's instructions. The eluted proteins were subjected to 7.5% SDS–PAGE under reducing conditions. For immunoblotting of AtMBD9, protein samples were loaded onto 7.5% SDS–PAGE and were electrically transferred at 50 V to a polyvinylidene difluoride (PVDF) membrane (Roche) for 3 h at 4ºC using the wet blot method. Histones were separated on 12.5% SDS–PAGE and transferred to a PVDF membrane (Roche) for 1 h using the same method. Membranes were probed with AtMBD9 antibodies, anti-acetyl-histone H3 or acetyl-histone H4 (Millipore, http://www.millipore.com), followed by horseradish peroxidase (POD)-conjugated goat anti-rabbit secondary antibody (1:5000; Sigma-Aldrich), developed using BM chemiluminescence Western blotting substrate (POD) (Roche) and exposed to highly sensitive ECL X-ray medical film (Kodak, http://www.kodak.com) to visualize bands.

Expression and purification of full-length AtMBD9 and *in vitro* activity assay

The full-length AtMBD9 recombinant protein was expressed and purified using a baculovirus IMPACT system (New England Biolabs). The *AtMBD9* cDNA was amplified by PCR using primer pair F-BacMBD9 (5′-GCTCTAGAATGGAACCCACTGATTCTACTAACGA-GC-3′) and R-BacMBD9 (5′-TTTTCCTTTTGCGGCCGCTGGATCCC-TCGGGT-3′). After digestion, the PCR products were cloned in-frame with the intein domain of the pVIC108 vector (New England Biolabs) at the *Xba*I and *Not*I sites. The recombinant plasmids were amplified in *E. coli* DH10B cells and used to transfect *Spodoptera frugiperda*-21 (Sf21) insect cells using the BacVector-3000 DNA kit (Novagen, http://splash.emdbiosciences.com). Protein purification was performed according to the protocols described by Pradhan *et al.* (1997) and Patnaik *et al.* (2004). Recombinant AtMBD9 was dialyzed twice overnight at 4ºC in a buffer containing 50 mM Tris, pH 7.5, 150 mM NaCl, 10 mM PMSF, 1 μM DTT, complete protease inhibitor cocktail tablets (Roche) and 50% v/v glycerol. The histone acetylation activity (HAT) of the recombinant protein was measured using a HAT activity colorimetric assay kit (Biovision, http://www.biovision.com).

DNA methylation analysis

The DNA global 5-methylcytosine content in the wild-type and *atmbd9* and transgenic lines was measured using a Methylamp global DNA methylation quantification kit (Epigentek, http://www.epigentek.com). Standard curves of the amount of the methylated DNA were generated using the kit's positive and negative controls. Methylated cytosines within *FLC* were identified using sodium bisulfite sequencing methodology. Genomic DNA for the variousgenotypes was treated using a EpiTect bisulfite kit (Qiagen). Subsequently, the *FLC* sequences were amplified by PCR using the treated DNA as template and the degenerated primer pairs listed in Table S2. The PCR products were cloned into pGEM®-T Vector (Promega, http://www.promega.com/), and at least 20 clones of each construct were sent for sequencing at the University of Guelph sequencing facilities. As a control reaction, the *FLC* DNA fragment was amplified from the genomic DNA by PCR, cloned into the pGEM T-easy vector, propagated in *E. coli* JM110 (*dam* and *dcm*) (Stratagene, http://www.stratagene.com/) and used in the sodium bisulfite reaction. For digestion with *Mcr*BC (New England Biolabs), DNA was treated according to the manufacturer's instructions, purified and used as a template in the PCR using FLT-1F and FLT-3R primers (Table S2).

Microarray hybridization and analysis

Gene expression analysis was carried out using Operon Arabidopsis genome oligo set version 3.0 (Operon, http://www.operon.com/) long-oligonucleotide microarrays purchased from the laboratory of Dr David Galbraith (Department of Plant Sciences, University of Arizona, http://www.ag.arizona.edu/microarray/). Microarray hybridization was performed as described by Bueso *et al.* (2007). The microarray expression data were normalized and statistically analyzed using GENESPRING GX 7.3.1 software (Agilent Technologies, http://www.home.agilent.com). The alteration in expression level of representative genes was verified by RT-PCR using primers shown in Table S3.

Quantitative RT-PCR

Total RNA was extracted from leaves as described above, and cDNA was synthesized using the AMV first-strand cDNA synthesis kit (Promega). Expression of *FLC* was detected by quantitative RT-PCR

using the method and primer pairs described by Peng *et al.* (2006). To analyze *AtMBD9* transcription by quantitative RT-PCR, the primers 5′-TGAGGAAGCTAAGAATGGATGT-3′ (forward) and 5′-CATGCCAGCAGGACTTATATC-3′ (reverse) were used.

ACKNOWLEDGEMENTS

This work was supported by the Natural Sciences and Engineering Research Council (NSERC) and the Ontario Research and Development Challenge Fund. We would like to thank Drs Joseph Colasanti, Yong-Mei Bi and David Guevara for their valuable comments on the manuscript, and Dr Peter J. Krell and his group for help with production of the recombinant protein in insect cells.

SUPPORTING INFORMATION

Additional Supporting Information may be found in the online version of this article:

Figure S1. *FLC* of the *atmb9* mutant lines has more DNA methylation than the wild-type.

Figure S2. *atmb9* mutant lines have more global DNA methylation than the wild-type.

Figure S3. Putative protein structure of AtMBD9 and the strategy used to produce the recombinant proteins *in vitro*.

Figure S4. DNA demethylation assay using the recombinant full-length AtMBD9 and the methylated CpG *FLC* DNA sequence amplified by PCR.

Figure S5. Functional categorization of the 333 genes differentially expressed in the *atmbd9-1*.

Figure S6. Relative expression level obtained using the RT-PCR of some representative genes differentially expressed in the *atmbd9-1* line.

Table S1. Genes that were differentially expressed in the *atmbd9-1* axillary buds.

Table S2. Primers used to amplify the *FLC* locus from sodium bisulfite-treated DNA.

Table S3. Primers used in RT-PCR.

Please note: Wiley-Blackwell are not responsible for the content or functionality of any supporting materials supplied by the authors. Any queries (other than missing material) should be directed to the corresponding author for the article.

REFERENCES

Abramoff, M.D., Magelhaes, P.J. and Ram, S.J. (2004) Image processing with ImageJ. *Biophotonics Int.* **11**, 36–42.

Agius, F., Kapoor, A. and Zhu, J.K. (2006) Role of the *Arabidopsis* DNA glycosylase/lyase ROS1 in active DNA demethylation. *Proc. Natl Acad. Sci. USA*, **103**, 11796–11801.

Allen, M.L. and Antoniou, M. (2007) Correlation of DNA methylation with histone modifications across the HNRPA2B1-CBX3 ubiquitously-acting chromatin open element (UCOE). *Epigenetics*, **2**, 227–236.

Ausin, I., Alonso-Blanco, C., Jarillo, J.A., Ruiz-Garcia, L. and Martinez-Zapater, J.M. (2004) Regulation of flowering time by FVE, a retinoblastoma-associated protein. *Nat. Genet.* **36**, 162–166.

Bastow, R., Mylne, J.S., Lister, C., Lippman, Z., Martienssen, R.A. and Dean, C. (2004) Vernalization requires epigenetic silencing of FLC by histone methylation. *Nature*, **427**, 164–167.

Belinsky, S.A., Klinge, D.M., Stidley, C.A., Issa, J.P., Herman, J.G., March, T.H. and Baylin, S.B. (2003) Inhibition of DNA methylation and histone deacetylation prevent murine lung cancer. *Cancer Res.* **63**, 7089–7093.

Berg, A., Meza, T.J., Mahic, M., Thorstensen, T., Kristiansen, K. and Aalen, R.B. (2003) Ten members of the *Arabidopsis* gene family encoding methyl-CpG-binding domain proteins are transcriptionally active and at least one, AtMBD11, is crucial for normal development. *Nucleic Acids Res.* **31**, 5291–5304.

Brock, M.V., Herman, J.G. and Baylin, S.B. (2007) Cancer as a manifestation of aberrant chromatin structure. *Cancer J.* **13**, 3–8.

Brownell, J.E., Mizzen, C.A. and Allis, C.D. (1999) An SDS-PAGE-based enzyme activity assay for the detection and identification of histone acetyltransferases. *Methods Mol. Biol.* **119**, 343–353.

Bueso, E., Alejandro, S., Carbonell, P., Perez-Amador, M.A., Fayos, J., Belles, J.M., Rodriguez, P.L. and Serrano, R. (2007) The lithium tolerance of the *Arabidopsis* cat2 mutant reveals a cross-talk between oxidative stress and ethylene. *Plant J.* **52**, 1052–1065.

Burn, J.E., Bagnall, D.J., Metzger, J.D., Dennis, E.S. and Peacock, W.J. (1993) DNA methylation, vernalization, and the initiation of flowering. *Proc. Natl Acad. Sci. USA*, **90**, 287–291.

Cutler, S.R., Ehrhardt, D.W., Griffitts, J.S. and Somerville, C.R. (2000) Random GFP::cDNA fusions enable visualization of subcellular structures in cells of Arabidopsis at a high frequency. *Proc. Natl. Acad. Sci. USA*, **97**, 3718–3723.

D'Alessio, A.C., Weaver, I.C. and Szyf, M. (2007) Acetylation-induced transcription is required for active DNA demethylation in methylation-silenced genes. *Mol. Cell. Biol.* **27**, 7462–7474.

Dhalluin, C., Carlson, J.E., Zeng, L., He, C., Aggarwal, A.K. and Zhou, M.M. (1999) Structure and ligand of a histone acetyltransferase bromodomain. *Nature*, **399**, 491–496.

Feng, Q. and Zhang, Y. (2001) The MeCP1 complex represses transcription through preferential binding, remodeling, and deacetylating methylated nucleosomes. *Genes Dev.* **15**, 827–832.

Finnegan, E.J., Genger, R.K., Kovac, K., Peacock, W.J. and Dennis, E.S. (1998) DNA methylation and the promotion of flowering by vernalization. *Proc. Natl Acad. Sci. USA*, **95**, 5824–5829.

Gillmor, C.S., Lukowitz, W., Brininstool, G., Sedbrook, J.C., Hamann, T., Poindexter, P. and Somerville, C. (2005) Glycosylphosphatidylinositol-anchored proteins are required for cell wall synthesis and morphogenesis in *Arabidopsis*. *Plant Cell*, **17**, 1128–1140.

Goodwin, G.H. and Nicolas, R.H. (2001) The BAH domain, polybromo and the RSC chromatin remodelling complex. *Gene*, **268**, 1–7.

Gruenbaum, Y., Naveh-Many, T., Cedar, H. and Razin, I. (1981) Sequence specificity of methylation in higher plant DNA. *Nature*, **292**, 860–862.

Haaf, T. (1995) The effects of 5-azacytidine and 5-azadeoxycytidine on chromosome structure and function: implications for methylation-associated cellular processes. *Pharmacol. Ther.* **65**, 19–46.

Hassan, A.H., Awad, S. and Prochasson, P. (2006) The Swi2/Snf2 bromodomain is required for the displacement of SAGA and the octamer transfer of SAGA-acetylated nucleosomes. *J. Biol. Chem.* **281**, 18126–18134.

He, Y., Michaels, S.D. and Amasino, R.M. (2003) Regulation of flowering time by histone acetylation in *Arabidopsis*. *Science*, **302**, 1751–1754.

He, Y., Doyle, M.R. and Amasino, R.M. (2004) PAF1-complex-mediated histone methylation of FLOWERING LOCUS C chromatin is required for the vernalization-responsive, winter-annual habit in *Arabidopsis*. *Genes Dev.* **18**, 2774–2784.

Hull, A.K., Vij, R. and Celenza, J.L. (2000) *Arabidopsis* cytochrome P450s that catalyze the first step of tryptophan-dependent indole-3-acetic acid biosynthesis. *Proc. Natl Acad. Sci. USA*, **97**, 2379–2384.

Issa, J.P. (2004) CpG island methylator phenotype in cancer. *Nat. Rev. Cancer* **4**, 988–993.

Jackson, J.P., Lindroth, A.M., Cao, X. and Jacobsen, S.E. (2002) Control of CpNpG DNA methylation by the KRYPTONITE histone H3 methyltransferase. *Nature*, **416**, 556–560.

Jackson, J.P., Johnson, L., Jasencakova, Z., Zhang, X., PerezBurgos, L., Singh, P.B., Cheng, X., Schubert, I., Jenuwein, T. and Jacobsen, S.E. (2004) Dimethylation of histone H3 lysine 9 is a critical mark for DNA methylation and gene silencing in *Arabidopsis thaliana*. *Chromosoma*, **112**, 308–315.

Johnson, K.D. and Bresnick, E.H. (2002) Dissecting long-range transcriptional mechanisms by chromatin immunoprecipitation. *Methods*, **26**, 27–36.

Jones, P.A. (1985) Altering gene expression with 5-azacytidine. *Cell*, **40**, 485–486.

Kakutani, T. (1997) Genetic characterization of late-flowering traits induced by DNA hypomethylation mutation in *Arabidopsis thaliana*. *Plant J.* **12**, 1447–1451.

Kakutani, T., Jeddeloh, J.A., Flowers, S.K., Munakata, K. and Richards, E.J. (1996) Developmental abnormalities and epimutations associated with

DNA hypomethylation mutations. *Proc. Natl Acad. Sci. USA*, **93**, 12406–12411.

Kankel, M.W., Ramsey, D.E., Stokes, T.L., Flowers, S.K., Haag, J.R., Jeddeloh, J.A., Riddle, N.C., Verbsky, M.L. and Richards, E.J. (2003) *Arabidopsis* MET1 cytosine methyltransferase mutants. *Genetics*, **163**, 1109–1122.

Liu, F., Quesada, V., Crevillen, P., Baurle, I., Swiezewski, S. and Dean, C. (2007) The *Arabidopsis* RNA-binding protein FCA requires a lysine-specific demethylase 1 homolog to downregulate FLC. *Mol. Cell*, **28**, 398–407.

Mathieu, O., Reinders, J., Caikovski, M., Smathajitt, C. and Paszkowski, J. (2007) Transgenerational stability of the *Arabidopsis* epigenome is coordinated by CG methylation. *Cell*, **130**, 851–862.

Michaels, S.D. and Amasino, R.M. (1999) FLOWERING LOCUS C encodes a novel MADS domain protein that acts as a repressor of flowering. *Plant Cell*, **11**, 949–956.

Michaels, S.D. and Amasino, R.M. (2001) Loss of FLOWERING LOCUS C activity eliminates the late-flowering phenotype of FRIGIDA and autonomous pathway mutations but not responsiveness to vernalization. *Plant Cell*, **13**, 935–941.

Mouradov, A., Cremer, F. and Coupland, G. (2002) Control of flowering time: interacting pathways as a basis for diversity. *Plant Cell*, **14**, 111–130.

Niu, L., Lu, F., Pei, Y., Liu, C. and Cao, X. (2007) Regulation of flowering time by the protein arginine methyltransferase AtPRMT10. *EMBO Rep.* **8**, 1190–1195.

Patnaik, D., Chin, H.G., Esteve, P.O., Benner, J., Jacobsen, S.E. and Pradhan, S. (2004) Substrate specificity and kinetic mechanism of mammalian G9a histone H3 methyltransferase. *J. Biol. Chem.* **279**, 53248–53258.

Peng, M., Cui, Y., Bi, Y.M. and Rothstein, S.J. (2006) AtMBD9: a protein with a methyl-CpG-binding domain regulates flowering time and shoot branching in *Arabidopsis*. *Plant J.* **46**, 282–296.

Pradhan, S., Talbot, D., Sha, M., Benner, J., Hornstra, L., Li, E., Jaenisch, R. and Roberts, R.J. (1997) Baculovirus-mediated expression and characterization of the full-length murine DNA methyltransferase. *Nucleic Acids Res.* **25**, 4666–4673.

Razin, A., Webb, C., Szyf, M., Yisraeli, J., Rosenthal, A., Naveh-Many, T., Sciaky-Gallili, N. and Cedar, H. (1984) Variations in DNA methylation during mouse cell differentiation *in vivo* and *in vitro*. *Proc. Natl Acad. Sci. USA*, **81**, 2275–2279.

Saze, H., Shiraishi, A., Miura, A. and Kakutani, T. (2008) Control of genic DNA methylation by a jmjC domain-containing protein in *Arabidopsis thaliana*. *Science*, **319**, 462–465.

Scebba, F., De Bastiani, M., Bernacchia, G., Andreucci, A., Galli, A. and Pitto, L. (2007) PRMT11: a new *Arabidopsis* MBD7 protein partner with arginine methyltransferase activity. *Plant J.* **52**, 210–222.

Schmitz, R.J., Sung, S. and Amasino, R.M. (2008) Histone arginine methylation is required for vernalization-induced epigenetic silencing of FLC in winter-annual *Arabidopsis thaliana*. *Proc. Natl Acad. Sci. USA*, **105**, 411–416.

Sheldon, C.C., Burn, J.E., Perez, P.P., Metzger, J., Edwards, J.A., Peacock, W.J. and Dennis, E.S. (1999) The FLF MADS box gene: a repressor of flowering in Arabidopsis regulated by vernalization and methylation. *Plant Cell*, **11**, 445–458.

Smith, D.E. and Fisher, P.A. (1984) Identification, developmental regulation, and response to heat shock of two antigenically related forms of a major nuclear envelope protein in Drosophila embryos: application of an improved method for affinity purification of antibodies using polypeptides immobilized on nitrocellulose blots. *J. Cell Biol.* **99**, 20–28.

Springer, N.M. and Kaeppler, S.M. (2005) Evolutionary divergence of monocot and dicot methyl-CpG-binding domain proteins. *Plant Physiol.* **138**, 92–104.

Sridhar, V.V., Kapoor, A., Zhang, K., Zhu, J., Zhou, T., Hasegawa, P.M., Bressan, R.A. and Zhu, J.K. (2007) Control of DNA methylation and heterochromatic silencing by histone H2B deubiquitination. *Nature*, **447**, 735–738.

Sung, S. and Amasino, R.M. (2004) Vernalization in *Arabidopsis thaliana* is mediated by the PHD finger protein VIN3. *Nature*, **427**, 159–164.

Tariq, M. and Paszkowski, J. (2004) DNA and histone methylation in plants. *Trends Genet.* **20**, 244–251.

Vaillant, I. and Paszkowski, J. (2007) Role of histone and DNA methylation in gene regulation. *Curr. Opin. Plant Biol.* **10**, 528–533.

Vincent, A., Perrais, M., Desseyn, J.L., Aubert, J.P., Pigny, P. and Van Seuningen, I. (2007) Epigenetic regulation (DNA methylation, histone modifications) of the 11p15 mucin genes (MUC2, MUC5AC, MUC5B, MUC6) in epithelial cancer cells. *Oncogene*, **26**, 6566–6576.

Vongs, A., Kakutani, T., Martienssen, R.A. and Richards, E.J. (1993) *Arabidopsis thaliana* DNA methylation mutants. *Science*, **260**, 1926–1928.

Wolffe, A.P. and Hayes, J.J. (1999) Chromatin disruption and modification. *Nucleic Acids Res.* **27**, 711–720.

Woo, H.R., Pontes, O., Pikaard, C.S. and Richards, E.J. (2007) VIM1, a methylcytosine-binding protein required for centromeric heterochromatinization. *Genes Dev.* **21**, 267–277.

Zemach, A. and Grafi, G. (2003) Characterization of *Arabidopsis thaliana* methyl-CpG-binding domain (MBD) proteins. *Plant J.* **34**, 565–572.

Zemach, A., Li, Y., Wayburn, B., Ben-Meir, H., Kiss, V., Avivi, Y., Kalchenko, V., Jacobsen, S.E. and Grafi, G. (2005) DDM1 binds *Arabidopsis* methyl-CpG binding domain proteins and affects their subnuclear localization. *Plant Cell*, **17**, 1549–1558.

Zhang, W., Lee, H.R., Koo, D.H. and Jiang, J. (2008) Epigenetic modification of centromeric chromatin: hypomethylation of DNA sequences in the CENH3-associated chromatin in *Arabidopsis thaliana* and maize. *Plant Cell*, **20**, 25–34.

Zhao, Z., Yu, Y., Meyer, D., Wu, C. and Shen, W.H. (2005) Prevention of early flowering by expression of FLOWERING LOCUS C requires methylation of histone H3 K36. *Nat. Cell Biol.* **7**, 1256–1260.

